part of the mean free path, 3.57×10^{-13} Ω cm, extrapolated from the acoustic measurements, is in agreement with the values given by the above authors. Resistivity measurements by Ottensmeyer *et al.*[9] on single crystals of aluminum of 99.995% purity over a temperature range from 4 to 90°K show two different temperature dependences; for $T<20$°K, the resistivity was found to vary as $T^{1.7}$, and for $T>20$°K, as $T^{3.55}$.

Recent measurements using an eddy-current method[10] by Zaroyiannopoulos[11] of the electrical resistivity of sample Al-2 show two different temperature dependences; for $T<20$°K, the resistivity varied as $T^{1.2}$, and for $T>20$°K, as $T^{2.1}$. The temperature range of this measurement was limited to 11–33°K by the high noise of the signal at temperatures below 11°K. The various measurements of the electrical resistivity of aluminum show two temperature dependences and are thus similar, except for the smaller exponents of temperature, to the results obtained by ultrasonic attenuation methods.

[9] F. P. Ottensmeyer, H. G. Bratsberg, G. M. Graham, and A. C. Hollis-Hallett, Can. J. Phys. **42**, 1007 (1964).
[10] C. P. Bean, R. W. Deblois, and L. B. Nesbitt, J. Appl. Phys. **30**, 1976 (1959).
[11] N. C. Zaroyiannopoulos, Tufts University (unpublished).

ACKNOWLEDGMENTS

The authors are grateful to N. Zaroyiannopoulos for the use of his measurements on the electrical resistivity of aluminum. The computations for this work were done at the Tufts University Computation Center.

PHYSICAL REVIEW VOLUME 183, NUMBER 3 15 JULY 1969

Energy Bands for Silver by the Augmented-Plane-Wave Method

SUSHMA BHATNAGAR
Department of Physics, Indian Institute of Technology, Kanpur, India
(Received 3 September 1968)

The band structure for silver is computed using the augmented-plane-wave method. The $E(\mathbf{k})$ values were computed for the equivalent of 2048 points in the Brillouin zone. The results are presented in the conventional manner. From these calculations the Fermi energy, Fermi surface, de Haas–van Alphen frequencies, and density of states were determined.

I. INTRODUCTION

IN this paper, the results of an augmented-plane-wave (APW) calculation of the band structure of silver are presented. The noble metals (copper, silver, and gold) are perhaps second in simplicity of electronic structure only to the alkali metals, and have been extensively studied experimentally. For this reason, detailed experimental data on the Fermi surfaces of these metals are available. This has stimulated considerable theoretical interest in calculations of the band structure of these metals. Tibbs[1] has calculated energy bands in copper and silver using the cellular method, but the boundary conditions were satisfied so inadequately that the results were not quantitatively accurate. After that, the cohesive energies of silver and gold were studied by Kambe[2] using the quantum defect method. In that work, the corrections for the departure of the potential from a simple Coulomb form near the cell boundary were determined from the results for copper, and may be somewhat inaccurate; there were also discrepancies between the theoretical and experimental results. The most recent calculations available for silver are those by Segall.[3] He has calculated $E(\mathbf{k})$ on the symmetry axis as well as at the symmetry points in the Brillouin zone, but he has not calculated $E(\mathbf{k})$ at a general point in the Brillouin zone. The extremely close agreement between the curves resulting from his calculations and those resulting from the author's calculations using the APW method reported in this paper confirms that the APW and the Green's-function methods are comparable in accuracy. The present calculation of the band structure enables a straightforward determination of the Fermi energy, Fermi surface, de Haas–van Alphen frequencies, and density of states.

II. CRYSTAL POTENTIAL

The APW method in its present form requires starting from a one-electron potential, which is spherically symmetric within spheres centered on atomic sites and constant in between. Inside the spheres this potential is constructed by superposing[4] atomic potentials centered on neighboring lattice sites. The atomic orbitals are solutions for the Hartree-Fock self-con-

[1] S. R. Tibbs, Proc. Cambridge Phil. Soc. **34**, 89 (1938).
[2] K. Kambe, Phys. Rev. **99**, 419 (1955).
[3] B. Segall, Report No. 6.1-RL-(2785G), 1961 (unpublished).
[4] L. F. Mattheiss, Phys. Rev. **133**, A1399 (1964).

TABLE I. One-electron potential in rydberg units. Values of r are in atomic units. The average potential in the region between the APW sphere and the Wigner-Seitz cell is -1.1183 Ry.

r	$V(r)$	r	$V(r)$
0.0050	18382.23438	1.0000	10.38472
0.0100	8978.99609	1.0400	9.42186
0.0150	5848.95563	1.0800	8.57135
0.0250	3354.87622	1.1200	7.81874
0.0300	2735.40228	1.1600	7.15110
0.0350	2295.10892	1.2000	6.55775
0.0400	1966.74675	1.2400	6.02913
0.0450	1712.95909	1.2800	5.55726
0.0500	1511.30107	1.3200	5.13500
0.0550	1347.45528	1.3600	4.75638
0.0600	1211.86510	1.4000	4.41606
0.0650	1097.91643	1.4400	4.10958
0.0700	1000.89931	1.4800	3.83297
0.0750	917.37498	1.5200	3.57817
0.0800	844.77251	1.5600	3.35626
0.0850	781.13611	1.6000	3.15064
0.0900	724.95052	1.6400	2.96364
0.0950	675.02128	1.6800	2.79323
0.1000	630.39497	1.7200	2.63787
0.1100	554.10957	1.7600	2.49592
0.1200	491.44229	1.8000	2.36607
0.1300	439.18385	1.8400	2.24711
0.1400	395.05294	1.8800	2.13810
0.1500	357.38751	1.9200	2.03809
0.1600	324.94709	1.9600	1.94626
0.1700	295.55152	2.0000	1.86185
0.1800	272.17643	2.0400	1.78440
0.1900	250.52693	2.0800	1.71319
0.2000	231.37485	2.1200	1.64777
0.2200	199.10684	2.1600	1.58766
0.2400	173.08967	2.2000	1.53254
0.2600	151.77303	2.2400	1.48198
0.2800	134.07695	2.2800	1.43569
0.3000	119.22521	2.3200	1.39336
0.3200	106.64185	2.3600	1.35480
0.3600	86.50759	2.4000	1.31974
0.4000	71.57196	2.4400	1.28795
0.4400	59.93806	2.4800	1.25928
0.4800	50.75189	2.5200	1.23355
0.5200	43.38349	2.5600	1.21060
0.5600	37.40828	2.6000	1.19031
0.6000	32.51763	2.6400	1.17254
0.6400	28.47099	2.6800	1.15716
0.6800	25.07995	2.7200	1.14409
0.7200	22.20268	2.7600	1.13331
0.7600	19.73044	2.8000	1.12467
0.8000	17.60418	2.8400	1.11804
0.8400	15.75137	2.8800	1.11344
0.8800	14.13469	2.9200	1.11078
0.9200	12.71930	2.9600	1.10995
0.9600	11.47728		

sistent field.[5] The superposing has been done in the present work by expanding the neutral-atom Coulomb potential and the charge densities of neighboring atoms about the origin, using Löwdin's alpha expansion method[6] and retaining only the $l=0$ (spherically symmetric) terms in that expansion. Slater's free-electron approximation[7] has been used in constructing the crystal exchange potential.

As the contributions to the crystal potential from a fifth neighbor were rather small compared to those from a fourth neighbor, the contributions up to the fourth neighbor has been included in the total crystal potential. It has also been observed that in the neighborhood of the Slater radius R_S, the contribution to the crystal potential from the exchange interaction starts dominating over the contribution due to the Coulomb interaction.

Between the spheres the potential is assumed to be a constant, which is chosen to be the average value of the potential (V_{av}) in the region between the spheres and the boundaries of the Wigner-Seitz cell. The crystal potential $V(\mathbf{r})$ is given as

$$V(\mathbf{r})=V_T(r), \quad r<R_S$$
$$=V_{\text{av}}, \quad r>R_S$$

where $V_T(r)$ is the spherically symmetric potential inside the spheres.

This crystal potential is listed in Table I. Table II contains the various parameters used in the present calculation.

The one-electron Schrödinger equation has been solved for this crystal potential using all angular momentum states up to $l=13$ in these calculations.

The computations have been done on IBM 7044 computer. Wood's[8] computer program, written for the IBM 709 and 7090 computers, has been adapted to the IBM 7044 computer.

III. ENERGY EIGENVALUES

The energy $E(\mathbf{k})$ is computed as a function of $\mathbf{k}$ for the equivalent of 2048 points of the Brillouin zone. These calculations were carried out for the six bands at, and immediately below the Fermi energy and for energies up to 3 Ry above the Fermi energy. The results are listed in Table III and IV. Plots of energy as a function of the wave vector along the lines of symmetry from the center to a boundary of the Brillouin zone are presented in Figs. 1 and 2. The bands are numbered consecutively as with increasing energy for fixed $\mathbf{k}$.

IV. FERMI ENERGY

In the case of silver, a sufficiently large energy gap between the bands arising from $1s$, $2s$, $2p$, $3s$, $3p$, $3d$, $4s$, and $4p$ states and those arising from $4d$ and $5s$ states suggests that we need consider only the bands arising from $4d$ and $5s$ states as the conduction bands.

TABLE II. Parameters of the calculation.

Lattice constant a	7.7112 a.u.
Sphere radius R_S	2.726 a.u.
π/a	0.407406 a.u.
Wigner-Seitz sphere radius	3.0135 a.u.

[5] F. Herman and S. Skillman, Atomic Structure Calculation, Prentice-Hall, N. J.
[6] P. O. Lowdin, Advan. Phys. **5**, 1 (1956).
[7] J. C. Slater, Phys. Rev. **81**, 385 (1951).
[8] J. H. Wood, APW Program Manual, Solid State Molecular Theory Group, MIT, Mass. (unpublished).

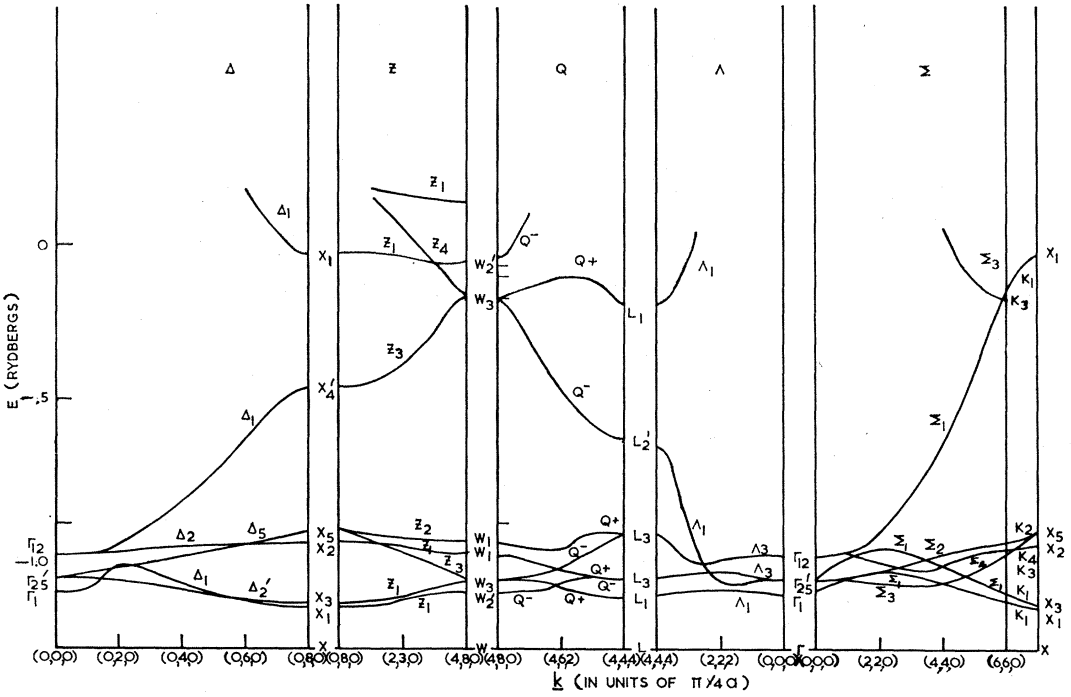

FIG. 1. Energy bands for silver.

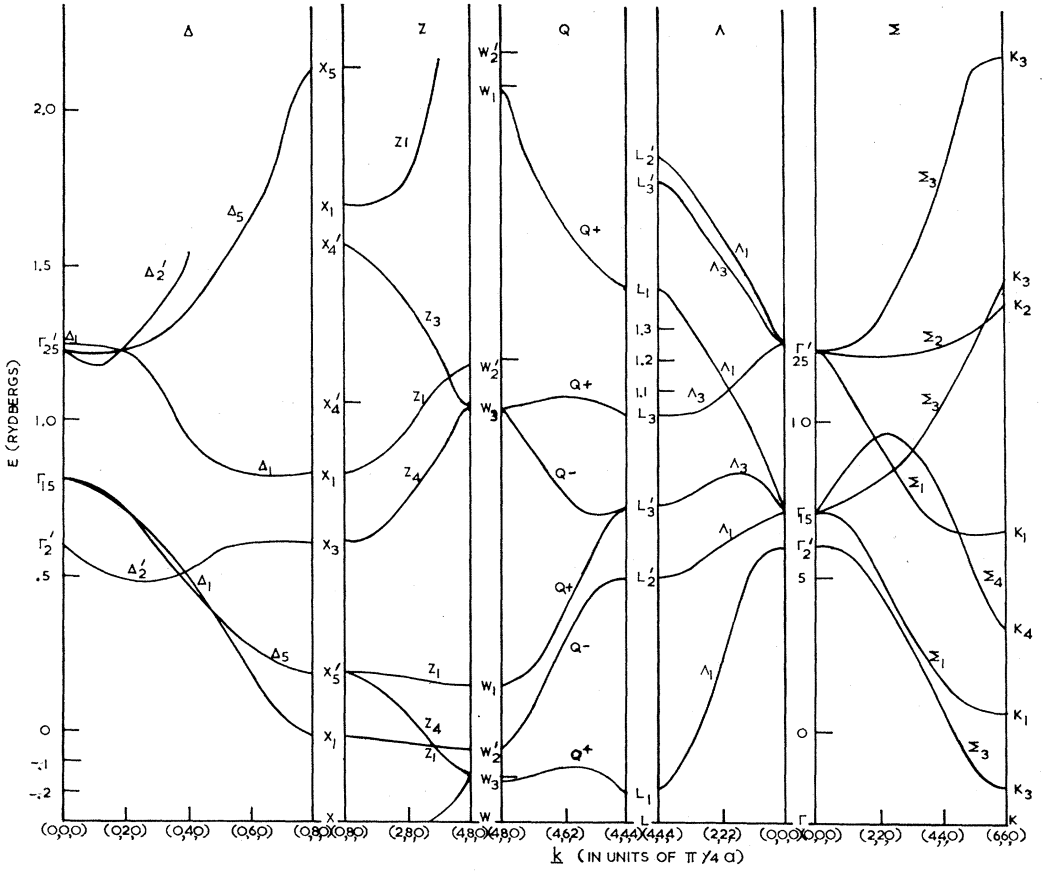

FIG. 2. Energy bands for silver—high-energy region.

TABLE III. $E(\mathbf{k})$ versus $\mathbf{k}$. The first column gives the BSW symbol (where appropriate); the second column specifies $\mathbf{k}$; the third and alternate columns, the irreducible representations appropriate for that eigenvalue; the fourth and alternate columns, the energy eigenvalues in rydbergs with respect to a zero constant potential between the spheres. To convert the tabulated energy values to values with respect to the zero of energy appropriate for the tabulated potential, one must subtract 1.1183 Ry from each. The values with asterisks are obtained from graphical interpolation.

		Band 1		Band 2		Band 3		Band 4		Band 5		Band 6	
BSW	4k	I.R.	E (Ry)	I.R.	E (Ry)	I.R.	E (Ry)	I.R.	E (Ry)	I.R.	E (Ry)	I.R.	E (Ry)
Γ	000	1	0.0002	25′	0.0511	25′	0.0511	25′	0.0511	12	0.1128	12	0.1128
Δ	010	1	0.0003	2′	0.0512	5	0.0564	5	0.0564	2	0.1168	1	0.1173
Δ	020	1	0.0896	2′	0.0382	5	0.0681	5	0.0681	2	0.1220	1	0.1517
Δ	030	1	0.0632	2′	0.0296	5	0.0868	5	0.0868	2	0.1412	1	0.2100
Δ	040	2′	0.0053	1	0.0299	5	0.1093	5	0.1093	2	0.1452	1	0.2865
Δ	050	2′	−0.0115	1	0.0037	5	0.1340	5	0.1340	2	0.1494	1	0.3783
Δ	060	2′	−0.0251	1	−0.0207	5	0.1517	5	0.1517	2	0.1516	1	0.4970
Δ	070	1	−0.0367	2′	−0.0339	2	0.1529	5	0.1570	5	0.1570	1	0.6015
X	080	1	−0.0446	3	−0.0394	2	0.1524	5	0.1960	5	0.1960	4′	0.6525
Σ	110	3	0.0479	2	0.0577	1	0.0583	1	0.1118	4	0.1312	1	0.1270
	120	+	0.0657	−	0.0679	+	0.0933	+	0.1198	+	0.1632	+	0.2386
	130	+	0.0679	+	0.0858	−	0.0864	+	0.1322	+	0.2201	+	0.2370
	140	+	0.0378	+	0.0925	−	0.1089	+	0.1414	+	0.2389	+	0.3050
	150	+	0.0085	+	0.1164	−	0.1338	+	0.1524	+	0.2387	+	0.4043
	160	+	−0.0160	+	0.1354	−	0.1562	+	0.1594	+	0.2387	+	0.5157
	170	−	−0.0296	+	0.1508	+	0.1636	−	0.1729	+	0.2387	+	0.6234
Z	180	1	−0.0386	4	−0.0322	1	0.1575	3	0.1651	2	0.1798	3	0.6775
Σ	220	3	0.0380	1	0.0630	2	0.0722	4	0.0986	1	0.1425	1	0.2004
	230	+	0.0644	+	0.0801	−	0.0876	+	0.1201	+	0.2391	+	0.2692
	240	+	0.0481	+	0.0750	−	0.1081	+	0.1326	+	0.2388	+	0.3475
	250	+	0.0217	+	0.0931	−	0.1327	+	0.1668	+	0.2383	+	0.4500
	260	−	−0.0064	+	0.1041	+	0.1487	−	0.1560	+	0.2387	+	0.5651
	270	−	−0.0139	+	0.1200	+	0.1475	−	0.1730	+	0.2387	+	0.6810
Z	280	1	−0.0253	4	−0.0165	3	0.1291	1	0.1438	2	0.1794	3	0.7436
Σ	330	3	0.0332	1	0.0545	4	0.0907	2	0.0946	1	0.1272	1	0.3037
	340	+	0.0466	+	0.0744	−	0.1101	+	0.1143	+	0.2388	+	0.4120
	350	+	0.0324	+	0.0665	−	0.1250	+	0.1325	+	0.2388	+	0.5149
	360	−	0.0161	+	0.0723	+	0.1296	−	0.1554	+	0.2387	+	0.6338
	370	−	0.0112	+	0.0812	+	0.1289	−	0.1726	+	0.2388	+	0.7590
Z	380	1	−0.0091	4	0.0085	3	0.0850	1	0.1272	2	0.1786	3	0.8433
Σ	440	1	0.0335	3	0.0383	1	0.0882	4	0.0916	2	0.1364	1	0.4951
	450	−	0.0451	+	0.0664	+	0.1051	−	0.1348	+	0.2388	+	0.5967
	460	−	0.0453	+	0.0509	+	0.1141	−	0.1553	+	0.2388	+	0.7151
	470	−	0.0445	+	0.0450	+	0.1180	−	0.1724	+	0.2388	+	0.8300
W	480	2′	−0.0028	3	0.0427	3	0.0427	1	0.1345	1′	0.1582	3	0.9437
Σ	550	1	0.0063	1	0.0543	3	0.0651	4	0.1279	2	0.1461	1	0.6941
	560	+	0.0326	−	0.0785	+	0.1171	−	0.1569	+	0.2388	+	0.8072
	570	+	0.0156	−	0.0842	+	0.1246	−	0.1724	+	0.2388	+	0.9100
K	660	1	−0.0254	1	−0.0039	3	0.1270	4	0.1401	2	0.1527	2	0.2101
Λ	111	1	0.0033*	1	0.0445	3	0.0602	3	0.0602	3	0.1033	3	0.1033
	121	+	0.0653	−	0.0682	+	0.0989	−	0.1221	+	0.1714	+	0.2386
	131	+	0.0246	+	0.0696	−	0.0797	+	0.0807	−	0.1339		
	141	+	0.0427	−	0.0966	+	0.0952	−	0.1466	+	0.2389	+	0.3172
	151	+	0.0143	−	0.1152	+	0.1157	−	0.1592	+	0.2388	+	0.4184
	161	+	−0.0089	−	0.1337	+	0.1357	−	0.1687	+	0.2388	+	0.5322
	171	+	−0.0222	−	0.1476	+	0.1505	−	0.1730	+	0.2388	+	0.6436
S	181	1	−0.0354	1	−0.0262	4	0.1461	3	0.1560	2	0.1740	2	0.2364
	221	+	0.0655	+	0.1183	−	0.0689	−	0.1082	+	0.2000	+	0.2383
	231		0.0639		0.0746		0.0952		0.1300		0.2397	+	0.2700
	241		0.0516		0.0791		0.0966		0.1453		0.2396	+	0.3543
	251		0.0275		0.0892		0.1127		0.1582		0.2396	+	0.4581
	261		0.0067		0.1037		0.1286		0.1651		0.2396	+	0.5763
	271		−0.0049		0.1179		0.1382		0.1704		0.2396	+	0.6966
	281	+	−0.0085	−	0.1248	+	0.1400	−	0.1730	+	0.2388	−	0.7647
	331	+	0.0573	−	0.0738	−	0.1136	+	0.1177	+	0.2389	+	0.3308
	341		0.0486		0.0768		0.1038		0.1340		0.2396	+	0.4144
	351		0.0384		0.0748		0.1073		0.1497		0.2396	+	0.5178
	361		0.0255		0.0763		0.1174		0.1606		0.2396	+	0.6375
	371		0.0172		0.0814		0.1234		0.1689		0.2396	+	0.7652
	381	+	0.0160*	−	0.0880*	+	0.1280*	−	0.1750*	+	0.2396*	+	0.8800*
	441	+	0.0413	−	0.0803	+	0.1044	−	0.1303	+	0.2388	+	0.4945
	451		0.0346		0.0815		0.0966		0.1444		0.2396	+	0.5927
	461		0.0303		0.0687		0.1062		0.1584		0.2396	+	0.7047
Q	471	−	0.0071	+	0.0355	−	0.0560	+	0.1002	+	0.1517	+	0.2016
	551	+	0.0420	+	0.0820	−	0.0958	−	0.1501	+	0.2388	+	0.6780
	561		0.0240*		0.0880*		0.0920*		0.1600*		0.2396*	+	0.7600*
Λ	222	1	0.0200	1	0.0483*	3	0.0653	3	0.0653	3	0.1056	3	0.1056
	232	+	0.0610	−	0.0665	+	0.1150	−	0.1418	+	0.2389	+	0.2923
	242	+	0.0502	−	0.0741	+	0.1037	−	0.1560	+	0.2388	+	0.3771

TABLE III (*continued*)

BSW	4k	Band 1 I.R.	Band 1 E (Ry)	Band 2 I.R.	Band 2 E (Ry)	Band 3 I.R.	Band 3 E (Ry)	Band 4 I.R.	Band 4 E (Ry)	Band 5 I.R.	Band 5 E (Ry)	Band 6 I.R.	Band 6 E (Ry)
	252	+	0.0372	−	0.0874	+	0.0974	−	0.1663	+	0.2388	+	0.4840
	262	+	0.0223	−	0.1040	+	0.1096	−	0.1693	+	0.2388	+	0.6056
	272	+	0.0132	−	0.1204	+	0.1057	−	0.1659	+	0.2388	+	0.7338
U	282	1	−0.0267*	1	−0.0117*	3	0.0983*	4	0.1283*	2	0.1483*	3	0.2533*
	332	+	0.0576	−	0.0611	−	0.1335	+	0.1402	+	0.2388	+	0.3441
	342		0.0496		0.0660		0.1232		0.1528		0.2396	+	0.4239
	352		0.0389		0.0767		0.1067		0.1622		0.2396	+	0.5250
	362		0.0314		0.0864		0.0985		0.1638		0.2396	+	0.6399
	372		0.0315		0.0814		0.1099		0.1604		0.2396	+	0.7519
	442	+	0.0451	−	0.0649	+	0.1330	−	0.1480	+	0.2388	+	0.4918
	452		0.0361		0.0740		0.1138		0.1576		0.2396	+	0.5751
Q	462	+	0.0161	−	0.0258	+	0.0898	−	0.0918	+	0.1502	+	0.2019
	552	+	0.0380*	−	0.0710*	−	0.1700*	+	0.1300*	+	0.2388*	+	0.6000*
Λ	333	1	−0.0039	3	0.0548	3	0.0548	3	0.1866	3	0.1866	1	0.2195
	343	+	0.0492	−	0.0569	+	0.1449	−	0.1626	+	0.2388	+	0.4471
	353	+	0.0420	−	0.0653	+	0.1274	−	0.1665	+	0.2388	+	0.5330
	363	+	0.0368	−	0.0793	+	0.1063	−	0.1613	+	0.2388	+	0.6202
	443	+	0.0481	−	0.0533	+	0.1554	−	0.1603	+	0.2388	+	0.4875
Q	453	+	0.0050	−	0.0424	+	0.0607	−	0.1404	+	0.2020	−	0.5367
L	444	1	−0.0145	3	0.0482	3	0.0482	3	0.1895	3	0.1895	2′	0.4853

Hence, the conduction bands must accommodate 11 electrons from each atom in the unit cell: ten $4d$ electrons and one $5s$ electron. The procedure for determining the Fermi energy is the same as that given by Burdick.[9] Hence, the first $5.5\times2048=11264$ energies will be occupied, and all above them will be unoccupied. Therefore, the Fermi energy will lie between energy number 11264 and energy number 11265. In the present case, both these energies happen to be the same and equal to −0.6005 Ry. Thus, the Fermi Energy $E_F=-0.6005$ Ry.

V. FERMI SURFACE

The Fermi surface (the constant-energy contour for $E=E_F$) is determined graphically by plotting $E(\mathbf{k})$ versus $\mathbf{k}$ in various directions. The intersections of the curves with $E=E_F$ line give the wave vector $\mathbf{k}_F$ to the Fermi surface. In the present calculations, these wave vectors are determined in two planes: the (100) plane and the (110) plane, and thus the E_F contours are determined in these two planes; they are shown in Figs. 3 and 4. The following conclusions may be drawn from the shape of these contours:

(a) As predicted by Segall,[3] the distortion of the belly is smaller than what has been observed in the case of copper.[9] The belly region deviates only very slightly from a spherical shape.

(b) There are contacts of the Fermi surface with the zone surface at the centers of the eight hexagonal faces.

The Fermi surface as computed here is in excellent qualitative agreement with the one calculated by Roaf[10] by fitting Shoenberg's[11] experimentally determined de Haas–van Alphen frequencies.

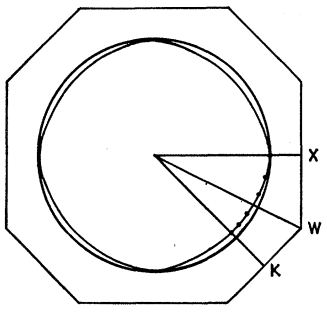

FIG. 3. (100) cross section of the Fermi surface. The circle represents the free-electron Fermi surface.

VI. DE HAAS-VAN ALPHEN FREQUENCIES

The de Haas–van Alphen frequencies can be predicted from the extremal areas A of the Fermi surface using the Onsager relation $F=KA$, where $K=Ch/2\pi e$. This gives F in gauss with A measured in atomic units.

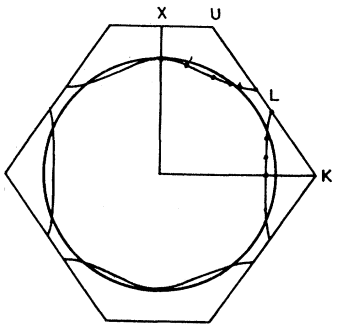

FIG. 4. (110) cross section of the Fermi surface. The circle represents the free-electron Fermi surface.

[9] G. A. Burdick, Phys. Rev. **129**, 138 (1963).

[10] D. J. Roaf, Phil. Trans. Roy. Soc. London **A255**, 135 (1962–63).

[11] D. Shoenberg, Phil. Trans. Roy. Soc. London **A255**, 85 (1962–63).

TABLE IV. $E(\mathbf{k})$ versus $\mathbf{k}$ for excited states, at symmetry points in the Brillouin zone. For detailed explanation see caption of Table III.

		Band 7		Band 8		Band 9		Band 10		Band 11		Band 12	
BSW	4k	I.R.	E (Ry)	I.R.	E (Ry)	I.R.	E (Ry)	I.R.	E (Ry)	I.R.	E (Ry)	I.R.	E (Ry)
Γ	000	2′	1.7183*	15	1.9527	15	1.9527	25′	2.3442	25′	2.3442	25′	2.3442
Δ	010	2′	1.6530	1	1.8985	5	1.9098	5	1.9098	2′	2.3013	5	2.3337
Δ	020	2′	1.7113	1	1.8177	5	1.8241	5	1.8241	1	2.3362	5	2.3430
Δ	030	2′	1.5950	5	1.7069	5	1.7069	1	1.7265	1	2.1683	5	2.3970
Δ	040	5	1.5846	5	1.5846	1	1.7076	2′	1.7169	1	2.0946	5	2.4933
Δ	050	1	1.4622	5	1.4744	5	1.4744	2′	1.7206	1	1.9738	5	2.6227
Δ	060	1	1.3001	5	1.3869	5	1.3869	2′	1.7242	1	1.9541	2	2.6961
Δ	070	1	1.1589	5	1.3305	5	1.3305	2′	1.7270	1	1.9538	2	2.6627
X	080	5′	1.3104	5′	1.3104	3	1.7226	1	1.9956	5′	2.0850	5′	2.0850
Z	180	4	1.2684	1	1.3020	4	1.7731	1	1.9955	3	2.6158	1	2.8289
Z	280	4	1.1724	1	1.2842	4	1.8793	3	2.4961	1	2.8307	3	2.8695
Z	380	1	1.2707	4	2.0146	1	2.2265	3	2.3321	3	2.8961	4	3.0183
W	480	1	1.2657	3	2.1665	2′	2.2982	1	2.7411	1	2.8219	3	2.9505
Q	471	−	1.2044	+	1.3365	−	2.0244	+	2.1811	−	2.4639	−	2.7414
Q	462	−	1.4052	+	1.5062	−	1.8719	−	1.9648	+	2.2059	−	2.4899
Q	453	−	1.5752	+	1.7132	−	1.8036	+	2.1938	−	2.2673	−	2.6262
L	444	2′	1.6197	3′	1.8446	3	2.1376	1	2.5465	1	2.8226	3′	2.8858
Λ	111	1	1.6574	1	1.7818	3	1.9486	3	1.9486	1	2.2197	3	2.3124
Λ	222	1	1.3574	1	1.7292	3	1.9440	3	1.9440	3	2.2028	3	2.2028
Λ	333	1	1.6538	3	1.8838	3	1.8838	3	2.1449	3	2.1449	1	2.3987
Σ	110	1	1.8040	3	1.8783*	3	1.8983	4	1.9806	1	2.2231	2	2.3419
Σ	220	3	1.5791	1	1.6012	3	1.9163	1	2.0354	4	2.0841	2	2.3356
Σ	330	3	1.3822	1	1.4232	1	1.8784	4	2.0266	3	2.0283	2	2.3385
Σ	440	3	1.1749	1	1.2847	1	1.7856	4	1.8143	3	2.1851	2	2.3621
Σ	550	1	1.2020	4	1.6174	1	1.7605	3	2.3723	2	2.4135	1	2.6466
K	660	1	1.1810	4	1.4567	1	1.7723	1	2.3366	2	2.4983	3	2.5896

		Band 13		Band 14		Band 15		Band 16		Band 17		Band 18	
BSW	4k	I.R.	E (Ry)	I.R.	E (Ry)	I.R.	E (Ry)	I.R.	E (Ry)	I.R.	E (Ry)	I.R.	E (Ry)
Δ	010	5	2.3337	1	2.3556	1	2.5836	5	2.7480	5	2.7480	1	2.8241
Δ	020	5	2.3430	1	2.3362	2′	2.4305	1	2.5647	1	2.8237	5	2.8802
Δ	030	5	2.3970	2′	2.4776	1	2.7466	1	2.8193	2	2.8848	5	3.0281
Δ	040	5	2.4933	2′	2.6684	2	2.8138	1	2.8287	1	2.9171	5	3.1650
Δ	050	5	2.6227	2	2.7483	1	2.8286	2′	2.8308	1	3.0319	5	3.2957
Δ	060	5	2.7787	5	2.7787	1	2.8286	2′	3.0090	1	3.0229		
Δ	070	1	2.8291	5	2.9507	5	2.9507	1	2.9857	2′	3.1772		
X	080	1	2.1434	4′	2.6896	1	2.8259	5′	3.1106	5′	3.1106	5	3.2573
Z	180	1	2.8289	3	2.9032	1	3.0419	4	3.0724	2	3.1556	2	3.2874
Z	280	1	2.9511	4	3.0686	2	3.1385	1	3.3048				
Z	380	2	3.0985	1	3.3062								
W	480	2	3.0839	1	3.3019	2′	3.3097						
Q	471	+	2.7460	+	2.8246	+	2.9397	−	3.2487	−	3.3003		
Q	462	−	2.6891	+	2.7635	−	3.0891	−	3.1502	+	3.2316		
Q	453	+	2.8463	−	2.8629	+	2.8693	−	2.9836	+	3.3040		
L	444	3′	2.8858	2′	2.9836								
Λ	111	1	2.5717	3	2.6178	3	2.6178	1	2.8440	1	2.8671	3	3.1394
Λ	222	1	2.2157	3	2.6524	3	2.6524	1	2.8302	1	2.9829	1	3.0684
Λ	333	3	2.7903	3	2.7903	1	2.8274	1	3.0707				
Σ	110	3	2.3656	1	2.4826	4	2.5430	1	2.7410	3	2.8047	1	2.8204
Σ	220	4	2.3227	3	2.4674	1	2.7289	3	3.0487	1	3.1021	4	3.3116
Σ	330	4	2.3281	3	2.6585	1	2.7675	1	2.8151	1	2.9759	3	3.3003
Σ	440	1	2.5361	4	2.5501	1	2.8341	1	2.9029	3	2.9269	1	2.9654
Σ	550	4	2.8089	1	2.8304	1	2.9086	1	3.1296	3	3.2779		
K	660	1	2.8275	1	2.9719	4	3.0209	1	3.1685	4	3.2960	3	3.3004

		Band 19		Band 20		Band 21		Band 22	
BSW	4k	I.R.	E (Ry)	I.R.	E (Ry)	I.R.	E (Ry)	I.R.	E (Ry)
Δ	010	2	2.9986	1	3.1158				
Δ	020	5	2.8802	2	2.9116	2	3.1495	1	3.2920
Δ	030	5	3.0281	2′	3.1570	1	3.3210		
Δ	040	5	3.1650						
Δ	050	5	3.2957						
X	080	5	3.2573						
Λ	222	3	3.2994	3	3.2994				
Σ	110	1	3.0501	4	3.1511				
Σ	330	1	3.2931						

TABLE V. de Haas–van Alphen frequencies.

Plane	F/F_s (present)	F/F_s (theoretical[a])	F/F_s (experimental[b])
(100)	0.940	0.9905	0.980±0.003
(110)	0.965	...	...

[a] See Ref. 10. [b] See Ref. 11.

To compare the results of the present calculation with Shoenberg's experimental results,[11] it is convenient to divide the values of F by F_s, the frequency for the spherical Fermi surface whose volume is exactly half of that of the first Brillouin zone. The ratio F/F_s is just the ratio A/A_s of the area of appropriate cross section of the Fermi surface to the diametrical cross-section area of the spherical Fermi surface and can be immediately compared with Shoenberg's results. These ratios are given in Table V.

VII. DENSITY OF STATES

The density-of-states curve is compiled from the energy eigenvalues computed for 2048 points in the first Brillouin zone, weighting each point according to both degeneracy and symmetry. A number of histograms are constructed by varying the bar width ΔE until the histogram acquires stability, in the sense that it does not change its form appreciably from one ΔE to the next. In the present calculations, a fairly stable histogram corresponds to $\Delta E=0.09$ Ry. This histogram and the resulting density-of-states curve are shown in Fig. 5.

The general features of this density-of-states curve are similar to those of the one estimated by Berglund and Spicer[12] from their photoemission study of silver.

VIII. DISCUSSION OF RESULTS AND COMPARISON WITH EXPERIMENT

As earlier stated by Segall,[3] the d bands are considerably more depressed relative to the conduction-band states than they are in the case of copper.[9,13] The exchange interaction is responsible for this type of lowering of the d bands. A point to be noted at this stage is that the energy bands for two fairly different potentials, that used by Segall[3] and that used by the author, have qualitative similarities. This is a clear indication of the fact that the bands are not too sensitive[14] to the details of the potential in the case of the noble metals.

The conduction-band states are more free-electron-like, and in particular the energies for the Σ_1, Δ_1, and Λ_1 conduction-band states for a given $|\mathbf{k}|$ are nearly equal, indicating that the bands are almost spherically symmetric.

[12] C. N. Berglund and W. E. Spicer, Phys. Rev. **136**, A1030 (1964).
[13] B. Segall, Phys. Rev. **125**, 109 (1962).
[14] L. F. Matthesis, Phys. Rev. **134**, A970 (1964).

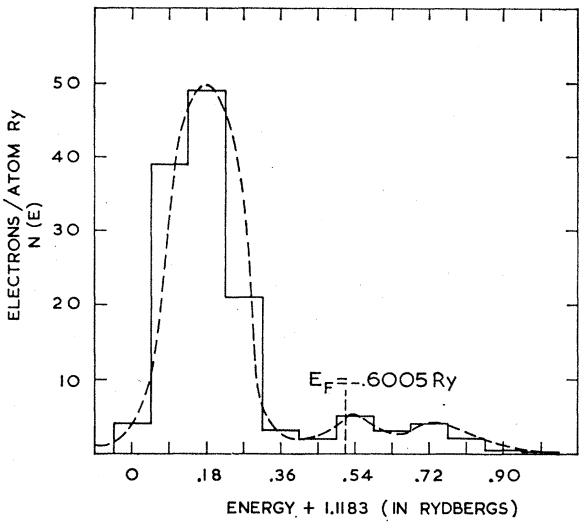

FIG. 5. Density-of-states curve for silver. Histogram constructed using $\Delta E=0.09$ Ry.

Table V indicates reasonable agreement between the value of F/F_s in the (100) plane calculated in this paper and the value calculated from experimental data by Shoenberg.[11] The difference in these two values is only 3.9%. This agreement is probably fortuitous, but may be attributable to the improved potential used in the Schrödinger equation in the present calculations.

The present density-of-states curve is in qualitative agreement with that of Berglund and Spicer.[12] They have observed two peaks in the density-of-states curve. The peak in the curve presented here corresponds to the second peak of their estimated curve. The shape of the present curve in the neighborhood of E_F is also in agreement with that given by Berglund and Spicer.[12]

Note added in manuscript. Further results on the band structure of silver have been given by Snow.[15] He has calculated the self-consistent energy bands for silver, using the APW method for a potential in which he has used the exchange correction as a parameter for fitting his results more accurately to the experimental results.

ACKNOWLEDGMENTS

It is with pleasure that the author acknowledges her indebtedness to Professor J. Mahanty for his interest in this problem, Dr. J. H. Wood for providing the computer program, Dr. B. Segall for giving his unpublished data, and Dr. L. F. Matheiss for the potential program. The author is very grateful to R. N. Basu for encouragement and invaluable help in computations. She further expresses her appreciation to S. K. Gupta and Miss A. Ghosh of the Saha Institute of Nuclear Physics, Calcutta, and to Dr. V. K. Tewary and R. Tewari for many useful discussions.

[15] E. C. Snow, Phys. Rev. **172**, 709 (1968).